

Tissue Border Enhancement by inversion recovery MRI at 7.0 Tesla

Mauro Costagli · Douglas A. C. Kelley · Mark R. Symms · Laura Biagi · Riccardo Stara · Eleonora Maggioni · Gianluigi Tiberi · Carmen Barba · Renzo Guerrini · Mirco Cosottini · Michela Tosetti

Received: 4 February 2014 / Accepted: 8 April 2014 / Published online: 25 April 2014
© Springer-Verlag Berlin Heidelberg 2014

Abstract

Introduction This contribution presents a magnetic resonance imaging (MRI) acquisition technique named Tissue Border Enhancement (TBE), whose purpose is to produce images with enhanced visualization of borders between two tissues of interest without any post-processing.

Methods The technique is based on an inversion recovery sequence that employs an appropriate inversion time to produce images where the interface between two tissues of interest is hypo-intense; therefore, tissue borders are clearly represented by dark lines. This effect is achieved by setting imaging parameters such that two neighboring tissues of interest have magnetization with equal magnitude but opposite sign; therefore, the voxels containing a mixture of each tissue (that is, the

tissue interface) possess minimal net signal. The technique was implemented on a 7.0 T MRI system.

Results This approach can assist the definition of tissue borders, such as that between cortical gray matter and white matter; therefore, it could facilitate segmentation procedures, which are often challenging on ultra-high-field systems due to inhomogeneous radiofrequency distribution. TBE allows delineating the contours of structural abnormalities, and its capabilities were demonstrated with patients with focal cortical dysplasia, gray matter heterotopia, and polymicrogyria.

Conclusion This technique provides a new type of image contrast and has several possible applications in basic neuroscience, neurogenetic research, and clinical practice, as it could improve the detection power of MRI in the characterization of cortical malformations, enhance the contour of small anatomical structures of interest, and facilitate cortical segmentation.

M. Costagli (✉) · R. Stara · G. Tiberi · M. Cosottini
Imago7 Foundation, Pisa, Italy
e-mail: mcostagli@imago7.eu

M. Costagli · L. Biagi · G. Tiberi · R. Guerrini · M. Tosetti
IRCCS Stella Maris, viale del Tirreno 331, Pisa, Italy

D. A. C. Kelley
GE Healthcare Technologies, San Francisco, CA, USA

M. R. Symms
GE Applied Science Laboratory, Pisa, Italy

R. Stara · M. Cosottini
University of Pisa, Pisa, Italy

E. Maggioni
IRCCS Scientific Institute E. Medea, Bosisio Parini, Lecco, Italy

E. Maggioni
Politecnico di Milano, Milan, Italy

C. Barba · R. Guerrini
Neuroscience Department, Children's Hospital
A. Meyer - University of Florence, Florence, Italy

Keywords Anatomical imaging · Inversion recovery · Tissue interface · Cortical malformations · Ultra-high-field MRI

Introduction

Inversion recovery (IR) preparation in magnetic resonance imaging (MRI) allows the suppression of undesired signal originating from one specific tissue by varying the time of inversion (TI): for example, in neuroimaging studies, fat is suppressed by using a short TI (STIR [1]), while cerebrospinal fluid (CSF) is suppressed by using a long TI (FLAIR [2]). This contribution presents an IR sequence that aims to produce images where the border between two tissues of interest is suppressed, appearing as a dark line. The appearance of hypo-intense lines at tissue interfaces is incidentally observed when the TI is systematically varied, as it is the case in longitudinal relaxation time T1-mapping techniques [3]: in the literature,

this phenomenon is referred to as bounce point artifact [4] and was used to assess the magnitude and distribution of partial volume effect in MRI [5]. The purpose of the approach presented here, which we will refer to as Tissue Border Enhancement (TBE), is to use this phenomenon to enhance the visualization of the borders of anatomical structures of interest, such as the interface between cortical gray matter (CGM) and white matter (WM). The development of this technique was motivated by the necessity to overcome some limitations that affect standard imaging protocols: especially on MR systems operating at high field, where the radiofrequency (RF) wavelength is comparable to the size of the object under investigation, images tend to exhibit undesired variations in intensity and tissue contrast [6–8]. New developments in multi-channel RF coils [9–11] used with parallel transmission [12, 13] and RF shimming [14, 15] have mitigated this issue; however, the complexity and cost of the hardware required necessitate that this technology is only slowly being introduced to all ultra-high-field systems. On the other hand, TBE employs a universally available IR sequence with operator-modified parameters and no sequence programming or dedicated hardware is required.

Methods

Theory and ex vivo acquisitions

The basis of TBE will be explained by means of the example depicted in Fig. 1. The same slice of an ex vivo human brain was repeatedly acquired with an MR950 7.0 T system (GE Healthcare, Milwaukee, WI, USA) equipped with a two-channel transmit/receive birdcage coil (Nova Medical, Wilmington, MA, USA). The TI of a spin-echo (SE) IR sequence was systematically varied between 70 and 2,000 ms (TI=70, 100, 150, 200, 250, 300, 400, 500, 600, 800, 1,000, 1,300, 1,600, 2,000 ms), while all other parameters were kept constant: time of repetition (TR)=3,000 ms, time of echo (TE)=10 ms, receiver bandwidth (RBW)=31.3 kHz, field of view (FOV)=160×160 mm², slice thickness=2 mm, and matrix size=128×128. By varying the TI, images were characterized by different contrasts, depending on the values of the magnetization of each tissue at different TI, as shown in the three examples depicted in Fig. 1a. Figure 1b illustrates the origin of the different voxel intensities in CGM and WM as a function of TI: the magnitude signal is always positive, while the longitudinal magnetization can be negative as well: the longitudinal magnetization of each tissue is zero at TI=TI_{null}, and for TI<TI_{null}, the longitudinal magnetization is negative, while for TI>TI_{null}, it is positive. If the TI is chosen such that two neighboring tissues have longitudinal magnetization with equal magnitude Δ but opposite sign (as it is the case, in our example, for CGM and WM at TI=200 ms), the voxels

containing an equal number of protons of each tissue will not provide any signal. In images acquired in this way, the voxels covering the border between the two tissues will be hypo-intense with respect to the two tissues (Fig. 1c). This technique can be applied to any desired couple of neighboring tissues, provided that they are characterized by different T1 relaxation times.

The optimal TI for TBE (which we will call TI_{TBE}) could be, in principle, computed numerically as a function of all other parameters, as shown in the “Appendix,” where it is demonstrated that TI_{TBE} depends not only on the tissue relaxation times (which in turn depend on static field B₀, temperature, etc.) but also on sequence parameters TR and TE. Due to the large amount of variables, it would always be preferable to calculate TI_{TBE} on the basis of repeated measurements with the same sequence parameters and varying TI, as in Fig. 1b, in order to account for effects that are possibly not represented in the analytical model. For the acquisition scheme of “fast” spin-echo inversion-recovery (FSE-IR), which is used in the in vivo acquisitions described below, actual measurements are necessary for choosing the proper TI_{TBE}; otherwise, the complexity of analytical approaches describing tissue magnetizations would increase unreasonably in order to take into account the influence of the train of 180° pulses and echoes occurring at different TEs. Other important factors that impose TI_{TBE} calculation via actual measurements instead of analytical/numerical approaches relate to the difference between nominal and actual RF pulses. The transmitted RF field B₁ is not homogeneous within the FOV, and this characteristic becomes more pronounced as the static magnetic field B₀ increases. Especially at ultra-high fields, nominal and actual flip angles may considerably differ in different regions of the FOV: for example, a pulse that is intended to act as an inversion pulse across the whole FOV may actually under-flip the magnetization in some regions, and over-flip it in others. Adiabatic inversion pulses are generally tolerant of B₁ variations only above a particular threshold; however, below the adiabatic threshold, these pulses are often quite sensitive to B₁ amplitude variations and B₀ variations [16].

In vivo acquisitions

MRI data were acquired on human volunteers, with the understanding and written consent from each subject in accordance with the protocol approved by the competent ethic committee, and in compliance with national legislation and the “Code of Ethical Principles for Medical Research Involving Human Subjects of the World Medical Association” (Declaration of Helsinki). In total, 13 subjects were scanned with the 7.0-T system, equipped with a 2-channel transmit/ 32-channel receive coil (Nova Medical, Wilmington, MA, USA). A FSE-IR sequence to depict the interface between WM and CGM in vivo was used with the following

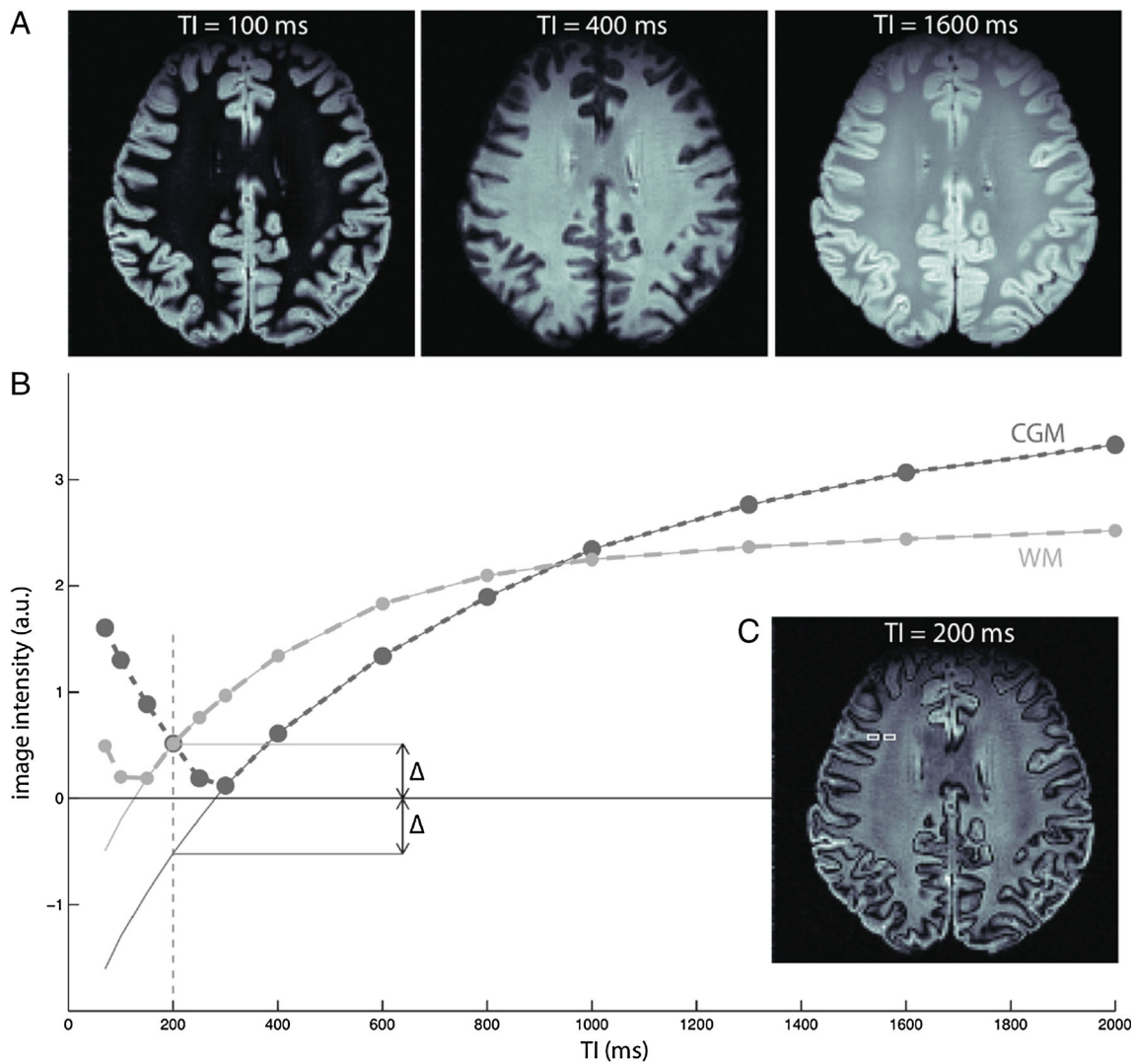


Fig. 1 The same slice of an ex vivo human brain acquired using a SE-IR sequence at 7.0 T with three different TI is represented in **a**. In **b**, image intensities of voxels of cortical gray matter (CGM, displayed in dark gray) and white matter (WM, light gray) for different TIs are represented by dots connected by thick broken lines. Polarity-restored data are depicted in thin lines and represent the magnetization of each tissue.

For TI=200 ms, the magnetizations of CGM and WM have approximately the same magnitude (Δ) and opposite sign. The image contrast obtained for TI=200 ms is represented in **c**. The white rectangles highlight the voxels (three for CGM and three for WM) whose intensities were averaged and used to construct the plot in **b**

parameters: TR=4,875 ms, echo train length (ETL)=9, nominal TE (nTE)=7.8 ms, FOV=220×220mm, matrix size=512×512, slice thickness=2 mm, spacing between slices=3.5 mm, RBW=62.5 kHz, and TI_{TBE}=700 ms. TI_{TBE} was chosen on the basis of repeated image acquisitions with varying TIs and otherwise identical parameters, as described above for the ex vivo sample.

Results

In this section, we present examples of TBE acquired on both healthy volunteers and patients using a 7.0-T MRI system.

Application of TBE in vivo

The TI_{TBE} calibration procedure for this sequence type (FSE-IR) and parameters (TR, ETL, nTE, RBW) was necessary only once, on one subject only. Once identified, the same TI was used for all other subjects: the same TBE phenomenon was observed in all of them, also at different spatial resolutions. Figure 2 displays one representative example of FSE-IR acquisition obtained in a healthy subject: the border between WM and CGM is precisely represented by hypo-intense voxels by using TI_{TBE}=700 ms. The duration of this sequence was 4'48" and allowed the acquisition of six axial slices with in-plane resolution=0.43×0.43 mm.

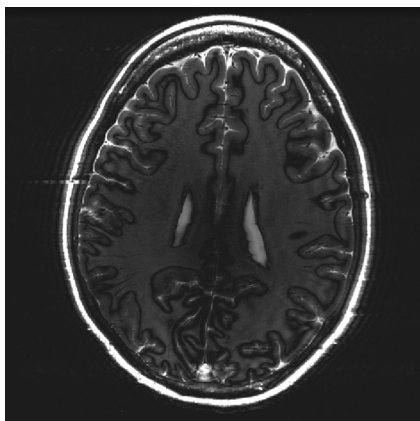


Fig. 2 Example of in vivo TBE acquisition at 7.0 T: the border between WM and CGM is precisely represented by a *black line*. TR=4,875 ms, nominal TE=7.8 ms, TI=700 ms, in-plane resolution=0.43×0.43 mm

Application I: highlighting the contour of structural abnormalities

Figure 3 illustrates that in the presence of structural abnormalities, TBE imaging could provide useful information in addition to those acquired by standard sequences. Images in Fig. 3 depict a patient with focal cortical dysplasia (white circle). In this type of structural abnormality, the main characteristic is disruption of cortical lamination with blurring of the gray-white matter junction [17]. As a consequence of this poor delineation, one of the main challenges for the neurosurgeon is the *as complete as possible* resection of the dysplastic area, which is considered an essential condition for achieving seizure freedom. TBE (Fig. 3a) helps define the border of the dysplastic tissue, which is often difficult to assess by visual inspection only, thereby adding useful detail to morphological inspection obtained with other available techniques (e.g., fast spoiled gradient recalled (FSPGR) echo, depicted in Fig. 3b).

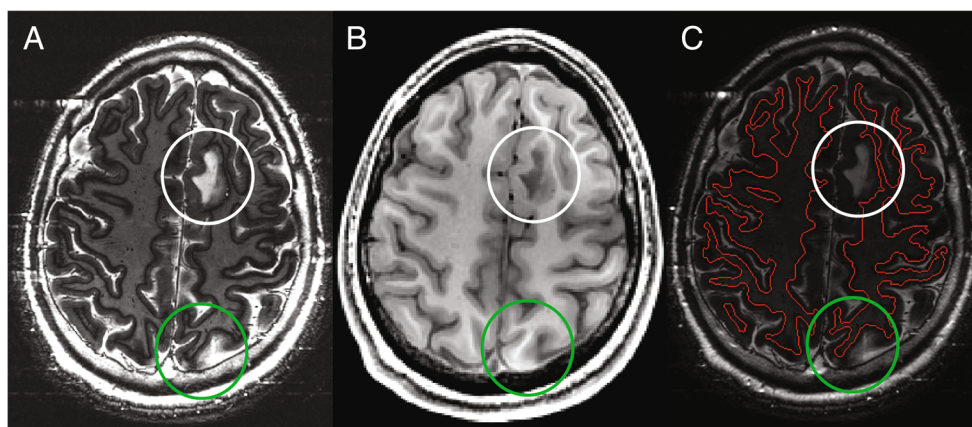


Fig. 3 TBE imaging provides useful information in addition to standard sequences. In TBE (a), the border between WM and CGM in a patient with focal cortical dysplasia (*white circle*) is precisely represented by a *black line*; for comparison, see the same slice acquired with a T1-

Application II: assisting segmentation

Besides studying the fine architecture of lesions and cortical abnormalities, another use of the new contrast provided by TBE images is in the field of automated detection of tissue interfaces and, therefore, segmentation of brain images. As shown in Figs. 3b and 4b, standard T1-weighted FSPGR data often provide poor contrast in the occipital cortex, especially on high-field MRI systems where inhomogeneities of the RF field and receiving coil profiles are present [6–8], and the border between WM and CGM is poorly delineated. In this case, a clear representation of the interface between the two tissues of interest would not be possible, and contrast-based algorithms for tissue segmentation would either fail or produce inaccurate results. On the other hand, TBE images accurately represent the WM-CGM interface (Figs. 3a and 4a) and can be used for automated detection of tissue interfaces and segmentation. In-house algorithms that rely on the hypo-intense representation of tissue borders in TBE (Fig. 3c) could provide a better segmentation than intensity-based algorithms and obviate the limitations inherent to ultra-high-field systems and multi-coil receiving arrays (e.g., in the area highlighted by green circles in Fig. 3 and enlarged in Fig. 4).

Application III: assisting clinical protocols studying cortical malformations

Figure 5a, c depict a patient with intractable epilepsy due to gray matter heterotopia. TBE clearly represents the borders of heterotopic cortex, including the identification of areas of merging with overlying normal cortex (indicated by pink arrow).

weighted FSPGR sequence (b). In-house algorithms, which rely on the hypo-intense representation of tissue borders provided by TBE, precisely detect the WM-CGM interface throughout the field of view (c, *red line*)

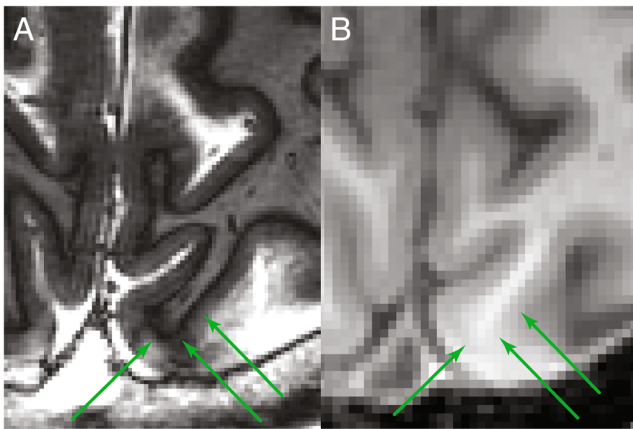


Fig. 4 Images **a** and **b** represent enlarged versions of the occipital cortex around the region indicated by *green circles* in Fig. 3. *Green arrows* indicate that TBE produces a clear CGM-WM delineation in regions where standard FSPGR provides ambiguous information

Another malformation of cortical development in which TBE might prove useful is polymicrogyria (Fig. 5b). In this malformation, the cortex exhibits a pebbled surface, with fusion of adjacent microgyri, and is thickened or thinned, often merging with normal cortex [18]. TBE provides a better depiction of cortical folding and the undulated profile of the WM-CGM junction with respect to T1-weighted FSPGR (Fig. 5d), thereby allowing a proper assessment of gyral shape and classification of the severity and extent of the malformation.

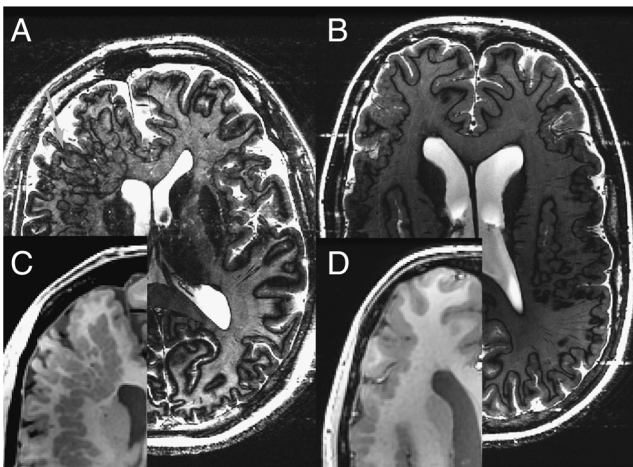


Fig. 5 Image **a** shows a TBE image of macronodular gray matter subcortical heterotopia involving the right frontal lobe. The borders of the irregularly distributed heterotopic cortex are clearly represented, including large contiguous nodules spanning from the ventricular wall to the cortical surface (*pink arrow*). Image **b** is taken from a patient with polymicrogyria using TBE. Here, TBE helps delineating the distribution of the malformation, which is often diffuse or has a patchy distribution with areas of cortical thickening and overfolding, adjacent to areas of thinning. Proper assessment of the abnormal morphology is essential for classifying the severity and extent of the malformation and differentiating it from other malformations of cortical development featuring abnormal cortical migration and layering. The *upper left portions* of images **a** and **b** are compared to FSPGR acquisitions in **c** and **d**, respectively

Discussion

The development of TBE was motivated by the necessity to overcome some limitations that affect standard imaging at high field, where images tend to exhibit undesired variations in intensity and tissue contrast [6–8]. A related approach, WM-nulling, has recently been demonstrated with magnetization prepared rapid acquisition gradient echo (MPRAGE) at 7.0 T to enhance intra-thalamic contrast but the authors reported some difficulties in mitigating blurring effects due to a distorted point-spread function [19]. An alternative technique has recently been proposed, based on the ratio of two image contrasts (MPRAGE and proton density gradient echo) interleaved within a single scan [20]. This sequence, named MP2RAGE [21], produces T1-weighted images with minimal inhomogeneity and has been proved useful in several applications [22–24]; however, it is not a product provided in all MRI scanners, and its implementation requires extensive programming.

On the contrary, TBE employs a universally available IR sequence with operator-modified parameters and no sequence programming is required. TBE allows for immediate, facilitated visualization of borders between two tissues of interest without any additional post-processing procedure; hence, “enhanced” images are immediately visible in real time. TBE can assist the interpretation of other standard sequences and might be employed to facilitate anatomical segmentation, brain morphometry, and measurements of cortical thickness. Moreover, this contribution suggests that TBE has the potential to improve detection power in cases of cortical atrophy and malformations of cortical development.

Limitations

It is worth considering potential limitations of this method: we demonstrated that TBE can perform better than standard gradient-echo sequences employed for assessing WM-CGM anatomy (Figs. 3, 4, and 5); however, inhomogeneities of the transmitted field B1 may lead to erroneous delineation of tissue interfaces. The issue of inhomogeneous B1 is common to all imaging sequences and is more pronounced at ultra-high fields than on standard systems and affects IR-prepared sequences in particular (including, for example, TBE, FLAIR, etc.) because both inversion and excitation pulses might differ from their nominal values. However, this issue was not observed in the acquisitions conducted in the present study.

Issues related to the specific absorption rate (SAR) must be taken into account, as well, mainly because of the presence of the inversion pulses. First-level controlled operating mode at 7.0 T may limit the number of slices: the MR system computes conservative estimates of the SAR through routines provided by the manufacturer, which guarantees patient safety. Recent methods for the estimation of SAR [25] suggest that these

default built-in calculations are actually over-conservative; therefore, power limitations might be relaxed in the future, should these new approaches to SAR calculation be approved for use in human experiments. Adopting parallel transmit technology might favor the implementation of TBE, as it might improve B1 homogeneity and reduce local SAR hot spots [12–15].

Finally, the results presented in this contribution are limited to 2D acquisitions. To obtain datasets with no spacing between slices, we propose the employment of a protocol that includes two separate scans that use identical parameters and with interleaved slice prescription for imaging a volume without any gap, which would also minimize cross talk [26]. Work is also underway to investigate a 3D implementation of TBE.

Applications

TBE has several possible applications in diagnostics and, as a consequence, in neurogenetic research and basic neuroscience. For instance, TBE can improve the ability of MRI in depicting the interface between white and gray matters by assisting the interpretation of standard imaging techniques, such as FSPGR, in anatomical regions characterized by poor contrast (Figs. 3 and 4). TBE has proved useful also in the fine assessment of the anatomy and extent of malformations of the cerebral cortex (Fig. 5). More accurate anatomic characterization in this category of patients translates into more accurate phenotyping that will in turn favor more meaningful genetic studies and subsequent functional studies [27].

Ad hoc image-processing algorithms that exploit this type of contrast are currently being optimized for computer-aided detection (CAD) of cortical atrophy and dysplasia. Reliable delineation of the borders of cortical dysplasia is of paramount importance for the accurate planning of invasive pre-surgical investigations in candidates for epilepsy surgery or, according to available clinical information, to reduce the need for invasive investigations by clearly demonstrating the limits of the anatomic area to be removed.

In gray matter heterotopia, TBE might find a role correctly delineating the borders of the macroscopic architecture of the cortical folding. The TBE capability to single out normally migrated cortex from subjacent islands of heterotopic gray matter might be particularly useful in the pre-surgical assessment of patients with nodular heterotopia and intractable focal seizures who are potential candidates for surgical treatment of epilepsy. In these patients, planning of the surgical strategy is particularly complex as the epileptogenic zone always includes heterotopic tissue as well as normally migrated cortex [28]. Since the functionally active areas of

representation for eloquent cortical function are unpredictably distributed between normally migrated and heterotopic gray matter [27], TBE in combination with functional MRI may improve delineating the distribution of eloquent cortex and planning invasive neurophysiological investigations, which are often necessary to guide excision of the epileptogenic tissue [28].

Accurate assessment of the morphological interface between gray and white matters is particularly important for classifying different malformations of cortical development such as, for example, pachygyria or polymicrogyria, for the purpose of genetic testing and counseling, and for planning molecular genetic investigations directed at identifying new causative genes [27].

Possible areas of future work could be the use of different TIs to enhance diverse tissue interfaces in pathological structures, such as tumors.

In conclusion, TBE could provide valuable additional information complementing those given by standard neuroimaging acquisition protocols. TBE enhances the contour of small anatomical structures of interest, facilitating their radiological identification, and it improves the detection power of MRI in the characterization of cortical malformations, as well as assisting segmentation.

Acknowledgments The authors would like to thank the nurse of the 7 T MR facility, Ms. Arianna Sugamoto, and all subjects who participated in this study. This work was supported by grant “Prog. 133/11” (to R.G.) approved by the Italian Ministry of Health and funded by Fondazione Pisa. The research leading to these results has received funding from the European Union Seventh Framework Programme FP7/2007-2013, project DESIRE (grant agreement no. 602531).

Ethical standards and patient consent We declare that all human and animal studies have been approved by the ethics committee of Pisa University General Hospital (Comitato Etico dell’Azienda Ospedaliero-Universitaria Pisana) and have therefore been performed in accordance with the ethical standards laid down in the 1964 Declaration of Helsinki and its later amendments. We declare that all patients gave informed consent prior to inclusion in this study.

Conflict of interest We declare that we have no conflict of interest.

Appendix

The optimal TI for TBE (TI_{TBE}) can be determined for any pair of neighboring tissues of interest by imposing the following relationship:

$$-S^{(1)}(TI_{TBE}) = S^{(2)}(TI_{TBE}) \quad (1)$$

where $S^{(1)}$ and $S^{(2)}$ are the polarity-restored signal intensities of the two tissues of interest. In the simplest scenario where a standard SE-IR sequence is employed

(as in the example in Fig. 1), the signal intensities can be approximated by the following:

$$S^{(1)} \propto PD^{(1)} \cdot \left(1 - 2e^{-T1/T1^{(1)}}\right) \left(1 - e^{-TR/T1^{(1)}}\right) \cdot e^{-TE/T2^{(1)}} \quad (2)$$

where $PD^{(1)}$, $T1^{(1)}$, and $T2^{(1)}$ indicate proton density, longitudinal relaxation time, and transverse relaxation time, respectively, of one of the two tissues. By substituting Eq. (2) into Eq. (1), it follows:

$$\begin{aligned} & -PD^{(1)} \cdot \left(1 - 2e^{-T1_{TBE}/T1^{(1)}}\right) \left(1 - e^{-TR/T1^{(1)}}\right) \cdot e^{-TE/T2^{(1)}} \quad (3) \\ & = PD^{(2)} \cdot \left(1 - 2e^{-T1_{TBE}/T1^{(2)}}\right) \left(1 - e^{-TR/T1^{(2)}}\right) \cdot e^{-TE/T2^{(2)}} \end{aligned}$$

where $^{(1)}$ and $^{(2)}$ refer to the two tissues of interest.

References

- Bydder GM, Young IR (1985) MR imaging: clinical use of the inversion recovery sequence. *J Comput Assist Tomogr* 9(4):659–675
- Hajnal JV, De Coene B, Lewis PD, Baudouin CJ, Cowan FM, Pennock JM, Young IR, Bydder GM (1992) High signal regions in normal white matter shown by heavily T2-weighted CSF nulled IR sequences. *J Comput Assist Tomogr* 16(4):506–513
- Gowland PA, Stevenson VL (2003) T1: the longitudinal relaxation time. In: Tofts P (ed) *Quantitative MRI of the brain*. John Wiley & Sons, pp 111–141
- Pusey E, Lufkin RB, Brown RK, Solomon MA, Stark DD, Tarr RW, Hanafee WN (1986) Magnetic resonance imaging artifacts: mechanism and clinical significance. *Radiographics* 6(5):891–911
- Simmons A, Barker GJ, Tofts PS, Gass A, Arridge SR (1994) A method for visualization of MRI partial volume regions—PAIR (PARTIAL volume sensitised inversion recovery imaging). *Magn Reson Imaging* 12(5):821–826
- Belaroussi B, Milles J, Carne S, Zhu YM, Benoit-Cattin H (2006) Intensity non-uniformity correction in MRI: existing methods and their validation. *Med Image Anal* 10(2):234–246
- Van de Moortele PF, Akgun C, Adriany G, Moeller S, Ritter J, Collins CM, Smith MB, Vaughan JT, Ugurbil K (2005) B(1) destructive interferences and spatial phase patterns at 7 T with a head transceiver array coil. *Magn Reson Med* 54(6):1503–1518
- Vaughan JT, Garwood M, Collins CM, Liu W, DelaBarre L, Adriany G, Andersen P, Merkle H, Goebel R, Smith MB, Ugurbil K (2001) 7 T vs. 4 T: RF power, homogeneity, and signal-to-noise comparison in head images. *Magn Reson Med* 46(1):24–30
- Van den Berg CA, van den Bergen B, Van de Kamer JB, Raaymakers BW, Kroeze H, Bartels LW, Lagendijk JJ (2007) Simultaneous B1+ homogenization and specific absorption rate hotspot suppression using a magnetic resonance phased array transmit coil. *Magn Reson Med* 57(3):577–586
- Adriany G, Van de Moortele PF, Ritter J, Moeller S, Auerbach EJ, Akgun C, Snyder CJ, Vaughan T, Ugurbil K (2008) A geometrically adjustable 16-channel transmit/receive transmission line array for improved RF efficiency and parallel imaging performance at 7 Tesla. *Magn Reson Med* 59(3):590–597
- Setsompop K, Alagappan V, Zelinski AC, Potthast A, Fontius U, Hebrank F, Schmitt F, Wald LL, Adalsteinsson E (2008) High-flip-angle slice-selective parallel RF transmission with 8 channels at 7 T. *J Magn Reson* 195(1):76–84
- Katscher U, Bornert P, Leussler C, van den Brink JS (2003) Transmit SENSE. *Magn Reson Med* 49(1):144–150
- Adriany G, Van de Moortele PF, Wiesinger F, Moeller S, Strupp JP, Andersen P, Snyder C, Zhang X, Chen W, Pruessmann KP, Boesiger P, Vaughan T, Ugurbil K (2005) Transmit and receive transmission line arrays for 7 Tesla parallel imaging. *Magn Reson Med* 53(2):434–445
- Mao W, Smith MB, Collins CM (2006) Exploring the limits of RF shimming for high-field MRI of the human head. *Magn Reson Med* 56(4):918–922
- Curtis AT, Gilbert KM, Klassen LM, Gati JS, Menon RS (2012) Slice-by-slice B1+ shimming at 7 T. *Magn Reson Med* 68(4):1109–1116
- Tannus A, Garwood M (1997) Adiabatic pulses. *NMR Biomed* 10(8):423–434
- Palmini A, Najm I, Avanzini G, Babb T, Guerrini R, Foldvary-Schaefer N, Jackson G, Luders HO, Prayson R, Spreafico R, Vinters HV (2004) Terminology and classification of the cortical dysplasias. *Neurology* 62(6 Suppl 3):S2–S8
- Barkovich AJ, Guerrini R, Kuzniecky RI, Jackson GD, Dobyns WB (2012) A developmental and genetic classification for malformations of cortical development: update 2012. *Brain* 135(Pt 5):1348–1369
- Tourdias T, Saranathan M, Levesque IR, Su J, Rutt BK (2014) Visualization of intra-thalamic nuclei with optimized white-matter-nulled MPRAGE at 7 T. *Neuroimage* 84:534–545
- Van de Moortele PF, Auerbach EJ, Olman C, Yacoub E, Ugurbil K, Moeller S (2009) T1 weighted brain images at 7 Tesla unbiased for Proton Density, T2* contrast and RF coil receive B1 sensitivity with simultaneous vessel visualization. *Neuroimage* 46(2):432–446
- Marques JP, Kober T, Krueger G, van der Zwaag W, Van de Moortele PF, Gruetter R (2010) MP2RAGE, a self bias-field corrected sequence for improved segmentation and T1-mapping at high field. *Neuroimage* 49(2):1271–1281
- Fujimoto K, Polimeni JR, van der Kouwe AJ, Reuter M, Kober T, Benner T, Fischl B, Wald LL (2014) Quantitative comparison of cortical surface reconstructions from MP2RAGE and multi-echo MPRAGE data at 3 and 7 T. *Neuroimage* 90:60–73
- Gizewski ER, Maderwald S, Linn J, Dassinger B, Bochmann K, Forsting M, Ladd ME (2014) High-resolution anatomy of the human brain stem using 7-T MRI: improved detection of inner structures and nerves? *Neuroradiology* 56(3):177–186
- Tanner M, Gambarota G, Kober T, Krueger G, Erritzoe D, Marques JP, Newbould R (2012) Fluid and white matter suppression with the MP2RAGE sequence. *J Magn Reson Imaging* 35(5):1063–1070
- Tiberi G, Costagli M, Stara R, Cosottini M, Tropp J, Tosetti M (2013) Electromagnetic characterization of an MR volume coil with multi-layered cylindrical load using a 2-D analytical approach. *J Magn Reson* 230:186–197
- Bernstein MA, King KF, Zhou XJ (2004) Signal acquisition and k-space sampling. In: *Handbook of MRI pulse sequences*. Elsevier, pp 367–442
- Guerrini R, Dobyns WB, Barkovich AJ (2008) Abnormal development of the human cerebral cortex: genetics, functional consequences and treatment options. *Trends Neurosci* 31(3):154–162
- Tassi L, Colombo N, Cossu M, Mai R, Francione S, Lo Russo G, Galli C, Bramero M, Battaglia G, Garbelli R, Meroni A, Spreafico R (2005) Electroclinical, MRI and neuropathological study of 10 patients with nodular heterotopia, with surgical outcomes. *Brain* 128(Pt 2):321–337